

Self-exciting point process modeling of conversation event sequences

Naoki Masuda and Taro Takaguchi and Nobuo Sato and Kazuo Yano

Abstract

Self-exciting processes of Hawkes type have been used to model various phenomena including earthquakes, neural activities, and views of online videos. Studies of temporal networks have revealed that sequences of social interevent times for individuals are highly bursty. We examine some basic properties of event sequences generated by the Hawkes self-exciting process to show that it generates bursty interevent times for a wide parameter range. Then, we fit the model to the data of conversation sequences recorded in company offices in Japan. In this way, we can estimate relative magnitudes of the self excitement, its temporal decay, and the base event rate independent of the self excitation. These variables highly depend on individuals. We also point out that the Hawkes model has an important limitation that the correlation in the interevent times and the burstiness cannot be independently modulated.

Naoki Masuda

Department of Mathematical Informatics, The University of Tokyo, 7-3-1 Hongo, Bunkyo, Tokyo 113-8656, Japan, e-mail: masuda@mist.i.u-tokyo.ac.jp

Taro Takaguchi

Department of Mathematical Informatics, The University of Tokyo, 7-3-1 Hongo, Bunkyo, Tokyo 113-8656, Japan, e-mail: taro_takaguchi@mist.i.u-tokyo.ac.jp

Nobuo Sato

Central Research Laboratory, Hitachi, Ltd., 1-280 Higashi-Koigakubo, Kokubunji-shi, Tokyo 185-8601, Japan, e-mail: nobuo.sato.jn@hitachi.com

Kazuo Yano

Central Research Laboratory, Hitachi, Ltd., 1-280 Higashi-Koigakubo, Kokubunji-shi, Tokyo 185-8601, Japan, e-mail: kazuo.yano.bb@hitachi.com

1 Introduction

1.1 Temporal Networks

Social networks, which specify the pairs of individuals that are directly connected and those that are not, are substrates of social interactions. An important caveat in the use of social networks for understanding social behavior is that the pair of directly connected individuals does not interact all the time. Social events between a pair of individuals, such as dialogues and transmission of email, are better described as a sequence of events, i.e., a collection of tagged event times, where the tag includes, for example, the identity of the two individuals, type of the event, duration, and content of dialogues. In fact, recent massive data, mostly online, and technological developments of recording devices for offline social interaction enable recording of social events with a higher temporal (and spatial) precision than before. Examples of data taken in this domain include calling activity [2], web recommendation writing [15], email traffic [1, 7, 22], online forum dealing with sexual escorts [32], human interactions in the real space [3, 16, 17, 33], to name a few. Transmission of infection or information may occur only during the period in which two individuals are involved in an event. A set of such event sequences among pairs of individuals are collectively called the temporal network [14], which is the focus of this volume. Computational models that generate realistic event sequences possessing properties such as those described in Secs. 1.2 and 1.3 would help us understand the nature of human communication behavior.

1.2 Long-tailed Interevent Time Distribution

In many empirical event sequences that we would like to model, interevent times are distributed according to a long-tailed distribution. The survivor functions (also called the complementary cumulative distributions) of IET (i.e., the probability that the IET is larger than a given value τ), are shown in Fig. 1 for two individuals in the data sets used in our previous study [33, 34] (see Sec. 4.1 for descriptions of the data).

Different mechanisms seem to explain the non-Poissonian behavior of the IET. A first mechanism that was discovered to generate power-law IET distributions is a priority queue model [1]. In this class of models, each task corresponding to an event carries a priority level and arrives at a queue. Then, the queue tends to execute tasks with high priority; tasks with low priority are made to wait for a long time before being executed. The priority queue model has also been extended to allow for interaction of two priority queues between a pair of interacting individuals [18, 23, 28, 38]. However, some types of social interaction including conversations may not proceed like a queue. Therefore, we attempt an alternative approach in the present chapter.

1.3 IET Correlation

Another facet of actual event sequences is that they often possess positive temporal correlation. In other words, a long (short) IET is likely to be followed by a long (short) IET. This is the case even if the effect of circadian fluctuations is removed from data [19]. Although there are various methods to measure temporal correlation of the IET [8, 19], here we show it by simply measuring the conditional mean IET defined by

$$\tau^{\text{next}}(\tau) \equiv \langle \tau_{i+1} \rangle_{\tau_i \leq \tau}, \quad (1)$$

where τ_i is the i th IET in a sequence, and $\langle \cdot \rangle$ represents the average. If the IET correlation is absent, $\tau^{\text{next}}(\tau)$ is independent of τ .

The values of τ^{next} are plotted against τ in Figs. 2(a), 2(b), and 2(c) for the conversation sequences used in Fig. 1, times of email sending and receiving in a university [6], and times of online sexual escorts by male individuals [32], respectively. We remark that long-tailed IET distributions are known for the email [1, 35] and sexual escort [32] data sets. The conditional mean IET τ^{next} increases with τ in Figs. 2(a) and 2(b). Therefore, adjacent IETs are positively correlated. In Fig. 2(c), τ^{next} decreases with τ for $\tau \leq 7$ and increases with τ for $\tau \geq 7$. Figure 2(c) suggests that those who have bought an escort tend to avoid buying a next escort within a week. This is directly shown in Fig. 2(d), which shows the IET distribution. However, adjacent IETs for the sexual escort data are positively correlated on a longer time scale (Fig. 2(c)).

In the discrete time model proposed in [10], the probability of an event occurrence decreases if events occurred too frequently in the recent past and increases if the time since the last event becomes long. Such a mechanism may generate positive IET correlation.

1.4 Self-excitatory Stochastic Processes

An alternative mechanism that yields positive IET correlation is self-excitation. The idea is that once an individual talks with somebody, the individual is excited to talk with somebody with a higher rate. Malmgren and coworkers developed such models and applied to data [21, 22].

In the cascading nonhomogeneous Poisson process proposed in [22], the authors assumed that the primary process is an inhomogeneous Poisson process with a periodic event rate. An event generated from the primary process is assumed to elevate the system to the active state and trigger cascades of activity. In other words, after a trigger event, a burst of events may ensue as a result of the Poisson process with a rate that is larger than the base rate of the primary process. The entire recording period is divided into alternately appearing intervals of the active state with a high event rate and the normal state with a low event rate by an adjustment of the position and number of intervals to yield a good fit to the data. As a result, the number of

events contained in a burst is shown to obey an approximate exponential distribution (also see [19], which shows that the number of events in a burst obeys a power law distribution; the definition of burst is different in the two papers). With a circadian and weekly rate modulation, the cascading nonhomogeneous Poisson process is capable of producing the long-tailed IET distributions observed in the data.

Their model has many parameters to be estimated. This is common to their another model proposed in [21]. In [21], letter writing activity of each renowned individual is fitted by a cascading Poisson process model. The time unit is set to a day. The two parameters, i.e., the base event rate and tendency to write an additional letter within a time unit, are estimated on the basis of the data. Because the different parameter values are assumed for different sections of the data, the number of the parameters in the model can be large. In the case of the letter correspondence by Einstein, data are collected over 54 years, and the two parameters are estimated for each year. Therefore, there are 108 parameters.

These models [21, 22] are quite successful in capturing properties of the real event sequences. Nevertheless, it may be also fruitful to consider a much simpler self-excitatory model as a complementary approach to capture the origins of bursts (Sec. 1.2) and IET correlation (Sec. 1.3) inherent in human behavior.

A simple two state model in which normal and excited states are assumed is proposed in [19]. The model is not a hidden Markov model because the probability of staying in the excited state becomes large as the number of events that have already occurred in the current burst increases. The model reproduces properties of the original data such as the power-law IET distribution and autocorrelation function. However, statistical methods to estimate the model parameters from the data were not presented [19].

1.5 Our Approach: Hawkes Process

In this chapter, we fit the self-excitatory point process model called the Hawkes process [11–13, 36] to the data recorded in company offices [33, 34, 37, 39] (also see Fig. 1 and Fig. 2(a)). A main benefit for using the Hawkes process is that it contains a small number of parameters and is mathematically tractable; the maximum likelihood (ML) method for inferring parameter values is established for some important special cases [29].

This chapter is organized as follows. In Sec. 2, we introduce the Hawkes model and recapitulate its basic mathematical properties. In Sec. 3, we numerically investigate properties of event sequences generated by the Hawkes process. In Sec. 4, we carry out the ML estimation of the parameters of the Hawkes model and compare the data and the estimated model. In Sec. 5, we discuss the results, with an emphasis on the limitation and possible extensions of the Hawkes model for better describing human data. Mathematical details are delegated to two Appendices.

2 Hawkes Process

The Hawkes process is a self-exciting point process model that is analytically tractable. It is an inhomogeneous Poisson process in which the instantaneous event rate depends on the history of the time series of events. It is not a renewal process. The event rate at time t , denoted by $\lambda(t)$ is given by

$$\lambda(t) = \nu + \sum_{i, t_i \leq t} \phi(t - t_i), \quad (2)$$

where t_i is the time of the i th event, and $\phi(t)$ is the memory kernel, i.e., the additional rate incurred by an event. The causality implies $\phi(t) = 0$ ($t < 0$).

The Hawkes process has been used for modeling, for example, seismological data [26, 36], video viewing activities [4, 24], neural spike trains [30], and genomic data [31]. For example, in [4], time series of views of different videos on YouTube were categorized into three classes, which were characterized by different $\phi(t)$ and different time-dependent versions of ν . The Hawkes process has also been used to construct a method to estimate the structure of neural networks from given spike trains [5], analyze auto and cross correlation in data recorded from mouse retina [20], and understand the correlation between the activities of different neurons in pulse-coupled model networks of excitatory and inhibitory neurons [30]. In [31], the Hawkes process is used to model stochastic occurrences of specific genes on DNA sequences. The method to estimate a piecewise linear $\phi(t)$ based on the least square error was presented.

Depending on applications, the memory kernel $\phi(t)$ has been assumed to be a hyperbolic (i.e., power law) function [4] or a superposition of the gamma function [26]. Nevertheless, in the present work, we simply set

$$\phi(t) = \alpha e^{-\beta t} (t \geq 0) \quad (3)$$

for the following reasons. First, it allows the ML estimation of the parameters α , β , and ν [29]. Second, the Hawkes process with Eq. (3) has a small number of parameters as compared to competitive models with self excitation [21, 22, 26, 27]. It should be noted that Eq. (3) indicates that the self-exciting effect of an event decays in time. It is contrasted with a previous model in which the self-exciting effect is constant for some time and then the event rate returns to the basal rate [22]. An example time course of the event rate $\lambda(t)$ and the corresponding event sequence are shown in Fig. 3.

We define cluster of events as the set of events that are triggered by a single event occurring at the basal rate ν . In other words, all the events in a cluster are descendants of the trigger event. The expected cluster size is given by [12, 36]

$$c = \int_0^{\infty} \phi(t) dt = \frac{1}{1 - \frac{\alpha}{\beta}}, \quad (4)$$

and the stationary event rate is given by

$$\bar{\lambda} = cv = \frac{v}{1 - \frac{\alpha}{\beta}}. \quad (5)$$

The convergence of the event rate requires $\alpha < \beta$.

3 Numerical Results for Statistics of IET

In this section, we numerically examine basic properties of the Hawkes process with the exponential memory kernel. To quantify the broadness of the IET distribution, we measure the coefficient of variation (CV), defined as the standard deviation of the IET divided by the mean of the IET as follows:

$$\text{CV} = \frac{\sqrt{\sum_{i=1}^N (\tau_i - \langle \tau \rangle)^2 / N}}{\langle \tau \rangle}, \quad (6)$$

where N is the number of IETs in a given sequence and $\langle \tau \rangle \equiv \sum_{i=1}^N \tau_i / N$ is the mean IET. It should be noted that $\langle \tau \rangle$ in the limit $N \rightarrow \infty$ is equal to $1/\bar{\lambda} = (1 - \alpha/\beta)/v$. The Poisson process yields $\text{CV} = 1$.

We also measure the correlation coefficient for the IET [8] defined as

$$\frac{\sum_{i=1}^{N-1} (\tau_i - \langle \tau \rangle)(\tau_{i+1} - \langle \tau \rangle) / (N-1)}{\sum_{i=1}^N (\tau_i - \langle \tau \rangle)^2 / N}. \quad (7)$$

The Hawkes process is invariant under the following rescaling of the time and parameter values: $Ct = t'$, $\alpha = C\alpha'$, $\beta = C\beta'$, and $v = Cv'$, where $C > 0$ is a constant. Therefore, we normalize the time by setting $v = 1$ and vary α and β . The values of CV, IET correlation, and mean cluster size c are invariant under this rescaling. For a given pair of α and β values, we generate a time series with 2×10^5 events using the method described in [25] and calculate the statistics of the IET.

The values of CV, IET correlation, and c (Eq. (4)) for various α and β values are shown in Fig. 4(a), Fig. 4(b), and Fig. 4(c), respectively. Although we can more theoretically calculate CV using the expression of the IET distribution [13] (also see Appendix 1 for details), it is numerically demanding to do so. Therefore, we resorted to direct numerical simulations. The data are present only in the region $\alpha < \beta$, where the Hawkes process does not explode.

Figure 4(a) indicates that the Hawkes process generates a wide range of CV. A large value of $\alpha/\beta (< 1)$ yields a large CV value. This is the case for both small and large α values. In Fig. 5, the survival function of the IET on the basis of 2×10^5 events is compared for different α and β values that satisfy $\beta = 1.1\alpha$ or 1.2α . Although the CV values are large, the IET distributions are consistently different from power law distributions. In particular, the IET distribution seems to be a superposition of multiple distributions with different time scales when α is large (Fig. 5(c)).

It should be noted that we assumed the exponential, not long-tailed, memory kernel (Eq. (3)).

Figure 4(b) indicates that a large α/β value also yields a large IET correlation. Once the event rate increases because of recent occurrences of other events, the following IET tends to be small. Therefore, strong self-excitation in the model (i.e., large α/β) is considered to cause large IET correlation. The strength of self-excitation can be also quantified by c . Figure 4(c) indicates that a large α/β tends to yield a large c .

Figures 4(a), 4(b), and 4(c) look similar, suggesting that the three quantities are correlated with each other.

4 Fitting the Hawkes Process to the Data

4.1 Data Sets

We analyze two data sets D_1 and D_2 of face-to-face interaction logs obtained from different company offices in Japan. World Signal Center, Hitachi, Ltd., Japan collected the data using the Business Microscope system developed by Hitachi, Ltd., Japan. For technical details concerning the data collection, see [33, 37, 39]. We previously analyzed the data using different methods [33, 34]. Data sets D_1 and D_2 consist of recordings from 163 individuals for 73 days and 211 individuals for 120 days, respectively. The two individuals are defined to be involved in a conversation event, simply called the event, if their modules exchange the IDs at least once in a minute. The module has other types of data that we do not use in the present study, such as the list of conversation partners and the duration of each event. In total, D_1 and D_2 contain 51,879 and 125,345 events, respectively.

4.2 Results of Fitting

For the entire sequence of event times obtained for each individual, we carry out the ML estimation of the parameters of the Hawkes process with the exponential memory kernel. It should be noted that we use the information about event times and not the duration of events or the partners' IDs. We slightly modify the ML method developed in [29] (see Appendix 2 for details).

The modification is concerned with the treatment of the data during the night. Our data are nonstationary owing to the circadian and weekly rhythms. Therefore, direct application of the Hawkes process, which is a stationary point process, is invalid. In the previous literature in which different models are investigated, these rhythms are explicitly modeled [9, 22] or treated by dynamically changing the time scale according to the event rate [18]. In contrast, we omit the night part of the data

from the analysis because our data are collected in company offices and therefore there is no event from late in the night through early in the morning.

In both data sets D_1 and D_2 , there is nobody in the office between four and six in the morning. Accordingly, we can partition the data into workdays without ambiguity. For each individual, we discard the workdays that contain less than 40 conversation events. We call a workday containing at least 40 events the valid day. Then, we define the first event in each valid day as trigger event and set $t = 0$. The following events on the same valid day are interpreted to be generated from the Hawkes process. The time of the last event denoted by t_{last} (denoted by $t_{N_d}^d$ in Appendix 2) is defined to be the end time of the valid day; it is necessary to specify t_{last} to apply the ML method (Appendix 2). The value of t_{last} depends on individuals even on the same day. The individual may stay in the office for a considerable amount of time after $t = t_{\text{last}}$ before leaving the office. This implies that the individual does not have conversations with others remaining in the office between $t = t_{\text{last}}$ and the time when the individual leaves the office. If this is the case, the fact that this individual does not have events for $t > t_{\text{last}}$ may affect the ML estimators. Nevertheless, we neglect this point. Finally, we obtain the likelihood of the series of events for an individual by multiplying the likelihood for all the valid days.

We apply the ML method to the individuals that possess at least 300 valid IETs (i.e., IETs derived from the valid days) during the entire period. This thresholding leaves 63 individuals in D_1 and 148 individuals in D_2 . We also exclude one individual in D_1 because the ML method does not converge for this individual.

The survivor function of the IET is compared between the data and the estimated Hawkes process in Fig. 6. The comparison is made for an individual in D_1 (Fig. 6(a)) and an individual in D_2 (Fig. 6(b)). We calculated the IET distribution for the estimated model using the theoretical method [13] (Appendix 1). The agreement between the IET distributions of the data and the estimated model is excellent.

To assess the quality of the fit at a population level, we compare three statistics of the IET between the data and model for different individuals. The relationship between the mean IET obtained from the data and that obtained from the estimated model, i.e., $1/\bar{\lambda} = (1 - \alpha/\beta)/\nu$, is shown in Fig. 7(a). For different individuals in both data sets, the mean IET is close between the data and the model. The Pearson correlation coefficient between the data and model are equal to 0.993 and 0.986 for D_1 and D_2 , respectively. However, the Hawkes process slightly underestimates the mean IET.

The CV values for the data and the estimated model are compared in Fig. 7(b). We calculated the CV values for the estimated model on the basis of 2×10^5 events that we obtained by simulating the Hawkes process with the ML estimators α , β , and ν . Although the CV can be theoretically calculated using the ML estimators (Appendix 1), we avoided doing so because the theoretical method is computationally too costly to be applied to all the individuals. Roughly speaking, the CV values obtained from the model are close to those of the data. The Pearson correlation coefficient between the data and model are equal to 0.832 and 0.936 for D_1 and D_2 , respectively.

The IET correlation of the data and that for the estimated model are compared in Fig. 7(c). We calculated the IET correlation for the estimated model by direct numerical simulations, as in the case of the CV. Figure 7(c) indicates that the Hawkes process does not reproduce the IET correlation for most individuals. The IET correlation for the estimated model is distributed in a much narrower range than that of the data. This is consistent with the finding that the CV and the IET correlation are positively correlated in the Hawkes process (Sec. 3). Because most individuals have the CV values larger than unity (Fig. 7(b)), the estimate of the IET correlation obtained by the model tends to be positive regardless of the estimated values of α , β , and ν . Figure 7(c) suggests that the Hawkes process with the exponential memory kernel is incapable of approximating the real data in terms of the IET correlation.

5 Discussion

We analyzed properties of the IET generated by the Hawkes process with an exponential memory kernel and then fitted the model to the face-to-face interaction logs obtained from company offices. The model successfully reproduced the data in terms of the IET distribution. However, the model does not explain the behavior of the IET correlation in the data.

This limitation may be because the effect of self-excitation is too strong in the Hawkes process; the event rate can be very large after a burst of events. To examine this issue, we carry out additional numerical simulations using a modified Hawkes model. We modify the model such that after each event that would increase the event rate by $\phi(0)$ in the original Hawkes process, we reset the event rate to the basal value ν with probability p . The original Hawkes process corresponds to $p = 0$. The CV and IET correlation for $p = 0.1$ and various values of α and β are shown in Figs. 8(a) and 8(b), respectively. The values of the CV and IET correlation for $p = 0.1$ are much smaller than those for $p = 0$ (Figs. 4(a) and 4(b)). This is because a burst, which increases the CV and IET correlation in the Hawkes model, is forced to terminate with probability p after each event in the modified model. The CV and IET correlation values for $(\alpha, \beta) = (0.2i, 0.2j)$, where $0 \leq i < j < 100$ are plotted in Fig. 4(c). For comparison, the corresponding results for $p = 0$ on the basis of the data used in Figs. 4(a) and 4(b) are also shown in the figure. The introduction of $p > 0$ does not decorrelate the CV and IET correlation. To explain the behavior of the IET correlation in the present data, we need different models. It seems that the IET correlation has not been discussed in the context of social interaction data, with a notable exception [19]. We are interested in the capabilities of alternative models [10, 21, 22] in reproducing the IET correlation in the data.

In the present study, we used the exponential memory kernel because it is analytically tractable and contains only three parameters. The original Hawkes process with other memory kernels has also been applied to data [4, 26]. The ML method is available also for this case [26]. Nevertheless, we suspect that self-excitation inherent in the Hawkes process induces both high CV and positive IET correlation for a

variety of memory kernels. Therefore, the use of different memory kernel may not improve the fit of the Hawkes process to our data in terms of the IET correlation.

Two-state models [19,21,22], in which events are produced at high and low rates in the excited and normal states, respectively, are also self-exciting. These models may be more realistic for social data than the standard Hawkes process used in this work in the sense that humans may not distinguish many different levels of self-excitation as is assumed in the Hawkes process. On the other hand, the Hawkes process with the exponential memory kernel is simpler than these models such that the ML methods are available and the parameters have simple physical meanings. Although the model by Malmgren and colleagues allows for the ML method [22], the method is quite complicated and contains many parameters. It may be desirable to develop two-state models that are simple and allow for statistical methods. Alternatively, it may be desirable to modify the Hawkes process to account for the behavior of the IET correlation in the real data.

We lack methods to compare the goodness of fit of different models, except that it is straightforward to test the validity of a model against the Poisson process (but see [22]). We need develop goodness of fit tests to compare the performance of models proposed in different papers.

Appendix 1: IET Distribution of the Hawkes Process

In this section, we explain the derivation of the IET distribution of the Hawkes process shown in [13]. Also see [36] for introduction to mathematical treatments of the Hawkes and related processes.

Consider a trigger event at $t = 0$ and the inhomogeneous Poisson process with rate function $\phi(t)$, i.e., the point process directly induced by the trigger event. The probability generating functional (PGFL) for this inhomogeneous Poisson process, denoted by H , is given by

$$\begin{aligned} H(z(\cdot)) &\equiv E \left(\prod_{i \geq 1} z(t_i) \right) \\ &= \exp \left\{ \int_0^\infty [z(t) - 1] \phi(t) dt \right\}, \end{aligned} \quad (8)$$

where $z(t)$ is a carrying function, and t_i is the time of the i th event. We define $t_0 = 0$.

The events at $t = t_i$ may induce further events. On the basis of Eq. (8), the PGFL for the inhomogeneous Poisson process including all the descendant events induced by a trigger event at $t = 0$, denoted by F , is given through the following recursive relation:

$$F(z(\cdot)) = z(0) \exp \left\{ \int_0^\infty [F(z_t(\cdot)) - 1] \phi(t) dt \right\}, \quad (9)$$

where $z_t(t') \equiv z(t' + t)$ is the time translation. On the right-hand side of Eq. (9), $z(0)$ accounts for the trigger event at $t = 0$, and $F(z_t(\cdot))$ accounts for the fact that an event triggered at time t initiates an inhomogeneous Poisson process with rate $\phi(t)$ on top of the other inhomogeneous Poisson processes going on.

We obtain the PGFL for the entire Hawkes process, denoted by G , by combining Eq. (9) and the PDFL of the homogeneous Poisson process with rate ν as follows:

$$G(z(\cdot)) = \exp \left\{ \int_{-\infty}^{\infty} \nu [F(z_t(\cdot)) - 1] dt \right\}. \quad (10)$$

We set $z(t) = \tilde{z}$ for $t_s \leq t \leq t_s + \Delta$ and $z(t) = 1$ otherwise. Then, $\pi(t_s, \Delta, \tilde{z}) \equiv F(z(\cdot))$ is the probability generating function (PGF) for the number of events in $[t_s, t_s + \Delta]$, with the carrying variable \tilde{z} , and

$$\pi(t_s - t, \Delta, \tilde{z}) = F(z_t(\cdot)) \quad (11)$$

is the PGF for the number of events in $[t_s - t, t_s - t + \Delta]$. Equation (9) is reduced to

$$\pi(t_s, \Delta, \tilde{z}) = \begin{cases} \exp \left\{ \int_0^{t_s + \Delta} [\pi(t_s - t, \Delta, \tilde{z}) - 1] \phi(t) dt \right\}, & t_s > 0, \\ \tilde{z} \exp \left\{ \int_0^{t_s + \Delta} [\pi(t_s - t, \Delta, \tilde{z}) - 1] \phi(t) dt \right\}, & -\Delta \leq t_s \leq 0, \\ 1, & t_s < -\Delta. \end{cases} \quad (12)$$

By setting $t_s = 0$ and combining Eqs. (10) and (11), we obtain the PGF for the number of events in $[0, \Delta]$ as

$$Q_\Delta(\tilde{z}) \equiv G(z(\cdot)) = \exp \left\{ \int_{-\infty}^{\Delta} \nu [\pi(-t, \Delta, \tilde{z}) - 1] dt \right\}. \quad (13)$$

In particular,

$$\tilde{\pi}(t_s, \Delta) \equiv \pi(t_s, \Delta, 0) \quad (14)$$

is the probability that there is no event in $[t_s, t_s + \Delta]$ for a cluster of events originating at $t = 0$. Using Eq. (12), we obtain

$$\tilde{\pi}(t_s, \Delta) = \begin{cases} \exp \left\{ \int_0^{t_s + \Delta} [\tilde{\pi}(t_s - t, \Delta) - 1] \phi(t) dt \right\}, & t_s > 0, \\ 0, & -\Delta \leq t_s \leq 0, \\ 1, & t_s < -\Delta. \end{cases} \quad (15)$$

By setting $\tilde{z} = 0$ in Eq. (13) and using Eq. (15), we obtain the survivor function of the forward recurrence time, i.e., time to the next event from arbitrary t , as follows:

$$Q_\Delta(0) = \Pr(\text{forward recurrence time} > \Delta) = \exp \left\{ -\nu \Delta - \nu \int_0^{\infty} [1 - \tilde{\pi}(t, \Delta)] dt \right\}, \quad (16)$$

where \Pr denotes probability. $Q_\Delta(0)$ is the probability that the Hawkes process does not have any event in $[0, \Delta]$.

Finally, the distribution of the interevent time τ is given in the form of survivor function as

$$\Pr(\tau > t) = -\frac{dQ_\Delta(0)(t)}{dt} \Big/ \bar{\lambda}, \quad (17)$$

where the stationary event rate $\bar{\lambda}$ is given by Eq. (5).

In the numerical simulations, we adopted the Simpson's rule for calculating integrals in Eqs. (15) and (16), and solved Eq. (15) by iteration.

We remark that integration of Eq. (17) by part leads to

$$\langle \tau \rangle = \frac{1}{\bar{\lambda}} \quad (18)$$

and

$$\langle \tau^2 \rangle = \frac{2}{\bar{\lambda}} \int_0^\infty Q_\Delta(0)(t) dt. \quad (19)$$

Equations (18) and (19) can serve to calculate the CV. However, we did not use them and obtained the CV by direct numerical simulations because calculating the CV via Eqs. (18) and (19) is time consuming.

Appendix 2: ML Method for the Hawkes Process

In this section, we explain a slightly modified version of the ML method for the Hawkes process with the exponential memory kernel originally proposed in [29].

We let the event times be $0 \leq t_1 \leq t_2 \leq \dots \leq t_N$. Different from the usual assumption of the continuous-time point process, we allow multiple events to occur at the same time (i.e., $t_i = t_{i+1}$). Such simultaneous events actually occur in our data because of the finite time resolution of one minute. Simultaneous events do not prevent the application of the ML method explained in the following.

For the exponential memory kernel given by Eq. (3), the event rate at time t is given by

$$\lambda(t) = \nu + \alpha \sum_{j=1}^{j_{\max}(t)} e^{-\beta(t-t_j)}, \quad (20)$$

where $j_{\max}(t)$ is the index of the last event before time t .

The likelihood of the event sequence during time period $[0, t_N]$, denoted by $L(t_1, \dots, t_N)$, is given by

$$L(t_1, \dots, t_N) = \exp\left(-\int_0^{t_N} \lambda(t) dt\right) \prod_{i=1}^N \lambda(t_i). \quad (21)$$

By substituting Eq. (20) in Eq. (21), we obtain the log likelihood for the original Hawkes process as follows [29]:

$$\log L(t_1, \dots, t_N) = -vt_N + \sum_{i=1}^N \frac{\alpha}{\beta} \left(e^{-\beta(t_N - t_i)} - 1 \right) + \sum_{i=1}^N \log(v + \alpha A(i)), \quad (22)$$

where

$$A(i) = \sum_{1 \leq j < i \leq N} e^{-\beta(t_i - t_j)}. \quad (23)$$

Exactly speaking, the point process for an individual for one workday begins when the individual has arrived in the office. Because we do not know when the point process begins, we assume that the first event of each day is a trigger event. In other words, we set $t_1 = 0$ and modify Eq. (22) as

$$\log L(t_1, \dots, t_N) = -vt_N + \sum_{i=1}^N \frac{\alpha}{\beta} \left(e^{-\beta(t_N - t_i)} - 1 \right) + \sum_{i=2}^N \log(v + \alpha A(i)). \quad (24)$$

For each individual, we use the days that have at least 40 events. We index such a valid day as $d = 1, 2, \dots, d_{\max}$. We denote the event times of valid day d by $0 = t_1^d \leq \dots \leq t_{N_d}^d$, where N_d is the number of events in valid day d . The log likelihood of the entire sequence is given by the summation of the log likelihood over all the valid days.

The partial derivatives of the log likelihood with respect to α , β , and v are originally derived in [29]. In the present case, they read

$$\frac{\partial \log L}{\partial \alpha} = \sum_{d=1}^{d_{\max}} \left\{ \sum_{i=1}^{N_d} \frac{1}{\beta} \left(e^{-\beta(t_{N_d}^d - t_i^d)} - 1 \right) + \sum_{i=2}^{N_d} \frac{A_d(i)}{v + \alpha A_d(i)} \right\}, \quad (25)$$

$$\begin{aligned} \frac{\partial \log L}{\partial \beta} = \sum_{d=1}^{d_{\max}} \left\{ -\alpha \sum_{i=1}^{N_d} \left[\frac{1}{\beta} (t_{N_d}^d - t_i^d) e^{-\beta(t_{N_d}^d - t_i^d)} + \frac{1}{\beta^2} \left(e^{-\beta(t_{N_d}^d - t_i^d)} - 1 \right) \right] - \right. \\ \left. \sum_{i=2}^{N_d} \frac{\alpha B_d(i)}{v + \alpha A_d(i)} \right\}, \end{aligned} \quad (26)$$

$$\frac{\partial \log L}{\partial v} = \sum_{d=1}^{d_{\max}} \left\{ -t_{N_d}^d + \sum_{i=2}^{N_d} \frac{1}{\mu + \alpha A_d(i)} \right\}, \quad (27)$$

where

$$A_d(i) = \sum_{1 \leq j < i \leq N_d} e^{-\beta(t_i^d - t_j^d)} \quad (28)$$

and

$$B_d(i) = \sum_{1 \leq j < i \leq N_d} (t_i^d - t_j^d) e^{-\beta(t_i^d - t_j^d)}. \quad (29)$$

We obtain the ML estimates by setting the left-hand sides of Eqs. (25), (26), and (27) to 0.

We carried out the gradient descent method to estimate α , β , and ν for each individual. We repeat the substitution

$$\alpha \leftarrow \alpha + \delta \frac{\partial \log L}{\partial \alpha}, \quad (30)$$

$$\beta \leftarrow \beta + \delta \frac{\partial \log L}{\partial \beta}, \quad (31)$$

$$\nu \leftarrow \nu + \delta \frac{\partial \log L}{\partial \nu}, \quad (32)$$

where we set $\delta = 10^{-2}$. For one individual in D_2 , the ML method does not converge with $\delta = 10^{-2}$. Because it converges with $\delta = 10^{-3}$, we used this value for this particular individual.

Because the likelihood may have multiple local maxima, we started the gradient descent method with two different initial conditions, i.e., $(\alpha, \beta, \nu) = (0.6, 1.2, 0.6)$ and $(12, 24, 12)$ [hr^{-1}]. We found that the final results corresponding to the two initial conditions were identical for each individual.

For the ML method, the Hessian of the log likelihood can be explicitly given and used in combination with the Newton method [29]. However, we found that the Newton method does not converge for many individuals compared to the simple gradient descent described above. Therefore, we did not use the Newton method.

Because $\alpha, \beta, \nu \geq 0$ and $\alpha < \beta$ are needed for the Hawkes process to be well defined, we forced the parameter values to satisfy these conditions. In each update step, if the updated α becomes less than 10^{-6} , we set $\alpha = 10^{-6}$. Similarly, if $\alpha < \beta$ is violated, we set $\beta = \alpha + 10^{-6}$. If $\nu < 10^{-6}$, we set $\nu = 10^{-6}$.

The temporal resolution of our data is a minute. We set the unit time for the ML method to an hour such that our data has a resolution of $1/60$ on this timescale. The data would be too discrete for the ML method to bear accurate results if we set the unit time for the ML method to a minute. We verified that the results little changed when we made the time unit larger than one hour.

Acknowledgements N. M. acknowledges the support provided through Grants-in-Aid for Scientific Research (No. 23681033, and Innovative Areas ‘‘Systems Molecular Ethology’’(No. 20115009)) from MEXT, Japan. T. T. acknowledges the support provided through Grants-in-Aid for Scientific Research (No. 10J06281) from JSPS, Japan.

References

1. Barabási, A.L.: The origin of bursts and heavy tails in human dynamics. *Nature* **435**, 207–211 (2005)
2. Candia, J., González, M.C., Wang, P., Schoenharl, T., Madey, G., Barabási, A.L.: Uncovering individual and collective human dynamics from mobile phone records. *J. Phys. A* **41**, 224015 (2008)

3. Cattuto, C., Van den Broeck, W., Barrat, A., Colizza, V., Pinton, J.F., Vespignani, A.: Dynamics of person-to-person interactions from distributed RFID sensor networks. *PLoS ONE* **5**, e11596 (2010)
4. Crane, R., Sornette, D.: Robust dynamic classes revealed by measuring the response function of a social system. *Proc. Natl. Acad. Sci. USA* **105**, 15649–15653 (2008)
5. Dahlhaus, R., Eichler, M., Sandkühler, J.: Identification of synaptic connections in neural ensembles by graphical models. *J. Neurosci. Methods* **77**, 93–107 (1997)
6. Ebel, H., Mielsch, L.I., Bornholdt, S.: Scale-free topology of e-mail networks. *Phys. Rev. E* **66**, 035103(R) (2002)
7. Eckmann, J.P., Moses, E., Sergi, D.: Entropy of dialogues creates coherent structures in e-mail traffic. *Proc. Natl. Acad. Sci. USA* **101**, 14333–14337 (2004)
8. Goh, K.I., Barabási, A.L.: Burstiness and memory in complex systems. *Europhys. Lett.* **81**, 48002 (2008)
9. González, M.C., Hidalgo, C.A., Barabási, A.L.: Understanding individual human mobility patterns. *Nature* **453**, 779–782 (2008)
10. Han, X.P., Zhou, T., Wang, B.H.: Modeling human dynamics with adaptive interest. *New J. Phys.* **10**, 073010 (2008)
11. Hawkes, A.G.: Point spectra of some mutually exciting point processes. *J. R. Stat. Soc. B* **33**, 438–443 (1971)
12. Hawkes, A.G.: Spectra of some self-exciting and mutually exciting point processes. *Biometrika* **58**, 83–90 (1971)
13. Hawkes, A.G., Oakes, D.: A cluster process representation of a self-exciting process. *J. Appl. Prob.* **11**, 493–503 (1974)
14. Holme, P., Saramäki, J.: Temporal networks. *Phys. Rep.* **519**, 97–125 (2012)
15. Iribarren, J.L., Moro, E.: Impact of human activity patterns on the dynamics of information diffusion. *Phys. Rev. Lett.* **103**, 038702 (2009)
16. Isella, L., Romano, M., Barrat, A., Cattuto, C., Colizza, V., Van den Broeck, W., Gesualdo, F., Pandolfi, E., Ravà, L., Rizzo, C., Tozzi, A.E.: Close encounters in a pediatric ward: measuring face-to-face proximity and mixing patterns with wearable sensors. *PLoS ONE* **6**, e17144 (2011)
17. Isella, L., Stehlé, J., Barrat, A., Cattuto, C., Pinton, J.F., Van den Broeck, W.: What's in a crowd? Analysis of face-to-face behavioral networks. *Journal of Theoretical Biology* **271**, 166–180 (2011)
18. Jo, H.H., Karsai, M., Kertész, J., Kaski, K.: Circadian pattern and burstiness in mobile phone communication. *New J. Phys.* **14**, 013055 (2012)
19. Karsai, M., Kaski, K., Barabási, A.L., Kertész, J.: Universal features of correlated bursty behaviour. *Sci. Rep.* **2**, 397 (2012)
20. Krumin, M., Reutsky, I., Shoham, S.: Correlation-based analysis and generation of multiple spike trains using Hawkes models with an exogenous input. *Frontiers in Comput. Neurosci.* **4**, 147 (2010)
21. Malmgren, R.D., Stouffer, D.B., Campanharo, A.S.L.O., Amaral, L.A.N.: On universality in human correspondence activity. *Science* **325**, 1696–1700 (2009)
22. Malmgren, R.D., Stouffer, D.B., Motter, A.E., Amaral, L.A.N.: A Poissonian explanation for heavy tails in e-mail communication. *Proc. Natl. Acad. Sci. USA* **105**, 18153–18158 (2008)
23. Min, B., Goh, K.I., Kim, I.M.: Waiting time dynamics of priority-queue networks. *Phys. Rev. E* **79**, 056110 (2009)
24. Mitchell, L., Cates, M.E.: Hawkes process as a model of social interactions: a view on video dynamics. *J. Phys. A* **43**, 045101 (2010)
25. Ogata, Y.: On Lewis' simulation method for point processes. *IEEE Trans. Info. Th.* **27**, 23–31 (1981)
26. Ogata, Y.: Seismicity analysis through point-process modeling: A review. *Pure Appl. Geophys.* **155**, 471–507 (1999)
27. Ogata, Y., Akaike, H.: On linear intensity models for mixed doubly stochastic Poisson and self-exciting Point-Processes. *J. R. Stat. Soc. B* **44**, 102–107 (1982)

28. Oliveira, J.G., Vazquez, A.: Impact of interactions on human dynamics. *Physica A* **388**, 187–192 (2009)
29. Ozaki, T.: Maximum likelihood estimation of Hawkes' self-exciting point processes. *Ann. Inst. Stat. Math.* **31**, 145–155 (1979)
30. Pernice, V., Staude, B., Cardanobile, S., Rotter, S.: How structure determines correlations in neuronal networks. *PLoS Comput. Biol.* **7**, e1002059 (2011)
31. Reynaud-Bouret, P., Schbath, S.: Adaptive estimation for Hawkes processes; application to genome analysis. *Ann. Stat.* **38**, 2781–2822 (2010)
32. Rocha, L.E.C., Liljeros, F., Holme, P.: Information dynamics shape the sexual networks of Internet-mediated prostitution. *Proc. Natl. Acad. Sci. USA* **107**, 5706–5711 (2010)
33. Takaguchi, T., Nakamura, M., Sato, N., Yano, K., Masuda, N.: Predictability of conversation partners. *Phys. Rev. X* **1**, 011008 (2011)
34. Takaguchi, T., Sato, N., Yano, K., Masuda, N.: Importance of individual events in temporal networks. *New J. Phys.* **14**, 093003 (2012)
35. Vázquez, A., Oliveira, J.G., Dezső, Z., Goh, K.I., Kondor, I., Barabási, A.L.: Modeling bursts and heavy tails in human dynamics. *Phys. Rev. E* **73**, 036127 (2006)
36. Vere-Jones, D.: Stochastic models for earthquake occurrence. *J. R. Stat. Soc. B* **32**, 1–62 (1970)
37. Wakisaka, Y., Ohkubo, N., Ara, K., Sato, N., Hayakawa, M., Tsuji, S., Horry, Y., Yano, K., Moriwaki, N.: Beam-scan sensor node: Reliable sensing of human interactions in organization. 2009 Sixth International Conference on Networked Sensing Systems (INSS), IEEE Press, Piscataway, NJ, USA, pp. 1–4 (2009)
38. Wu, Y., Zhou, C., Xiao, J., Kurths, J., Schellnhuber, H.J.: Evidence for a bimodal distribution in human communication. *Proc. Natl. Acad. Sci. USA* **107**, 18803–18808 (2010)
39. Yano, K., Ara, K., Moriwaki, N., Kuriyama, H.: Measurement of human behavior: creating a society for discovering opportunities. *Hitachi Rev.* **58**, 139–144 (2009)

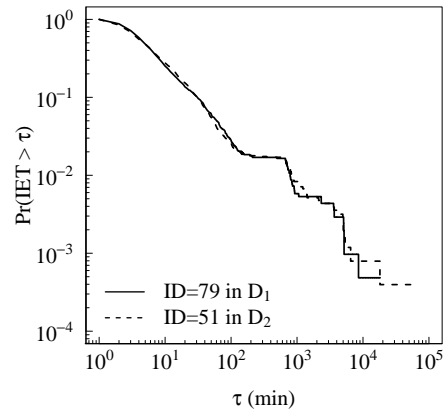


Fig. 1 Survivor functions of the IET (i.e., probability that the IET is larger than τ) for the conversation sequences of two individuals. For each of D_1 and D_2 , the individual with the largest number of events is selected. The selected individuals in D_1 and D_2 have 2,397 and 2,886 events, respectively.

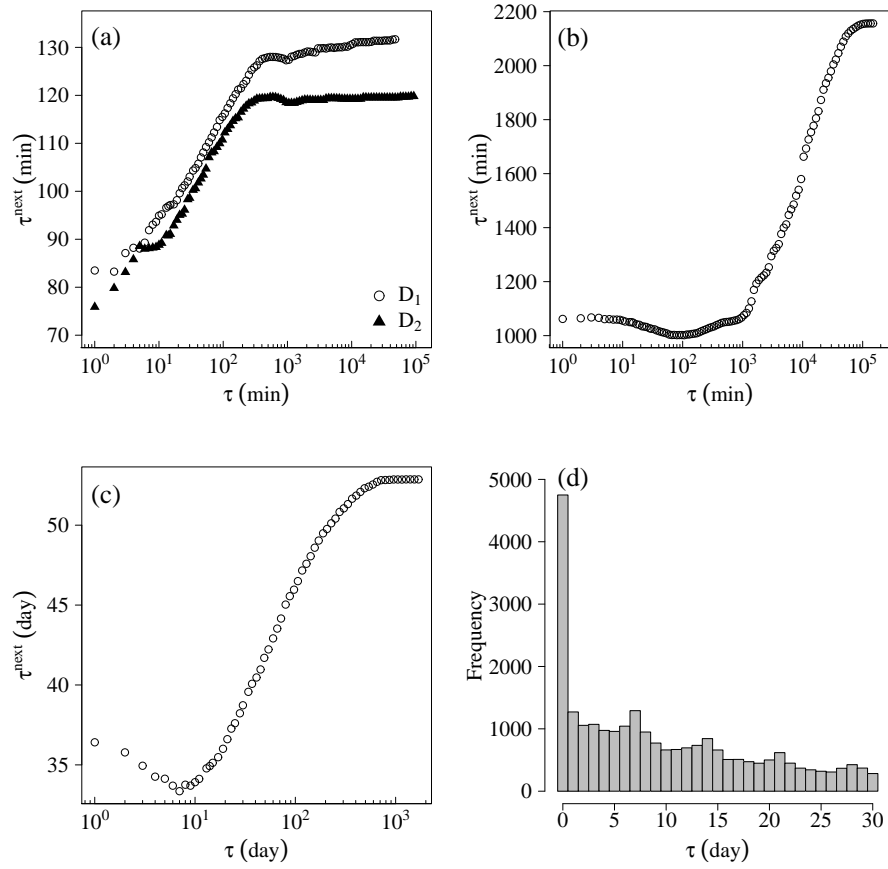


Fig. 2 Conditional mean IET defined by Eq. (1) for (a) conversation event sequences [33], (b) email logs [6], and (c) purchase of sexual escorts [32]. (d) Histogram of the IET for the data shown in (c).

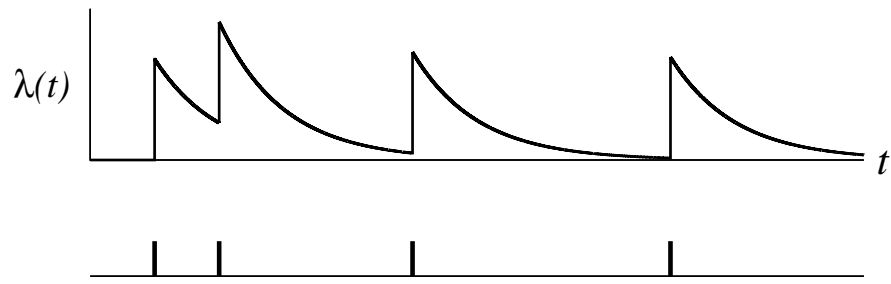


Fig. 3 Example time course of event rate $\lambda(t)$ and the corresponding event sequence.

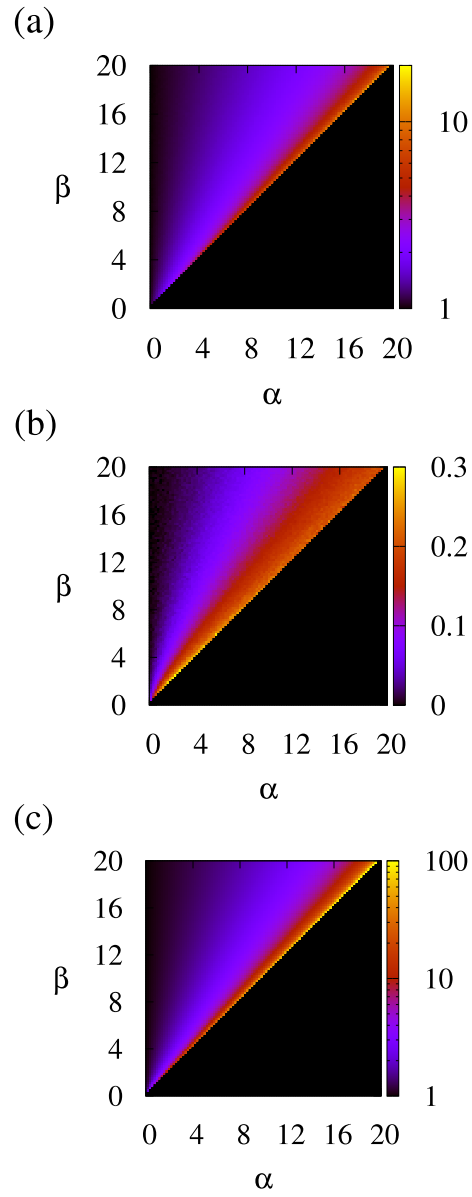


Fig. 4 Statistics of the IET obtained from the Hawkes process. (a) CV, (b) IET correlation, and (c) mean cluster size c for various values of α and β .

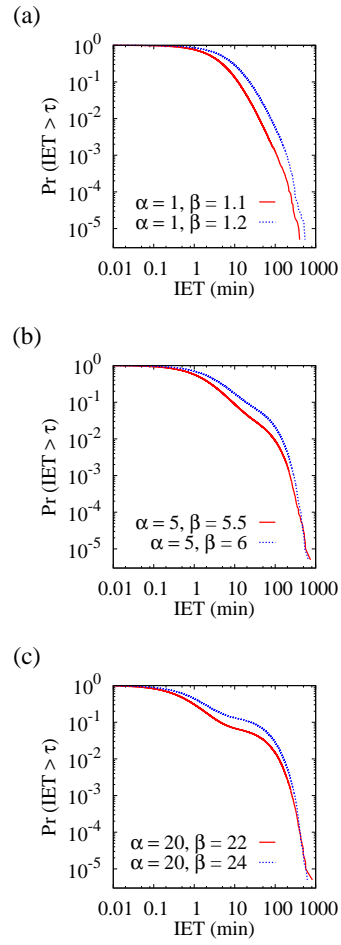


Fig. 5 Survivor functions of the IET for the Hawkes process with different values of α and β .

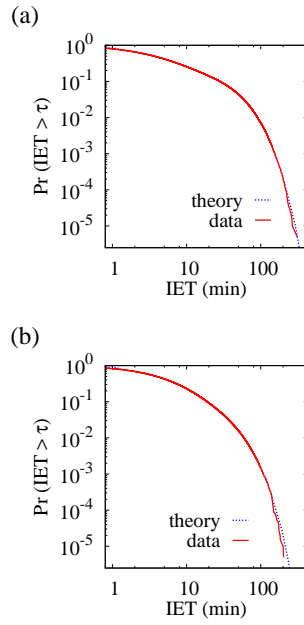


Fig. 6 Survivor functions of the IET for two individuals. (a) Results for an individual in D_1 , who has 1694 valid IETs during the recording period. The ML estimators are given by $\alpha = 4.91$, $\beta = 7.89$, and $\nu = 2.18$. (b) Results for an individual in D_1 , who has 1765 valid IETs. The ML estimators are given by $\alpha = 2.45$, $\beta = 3.86$, and $\nu = 2.77$.

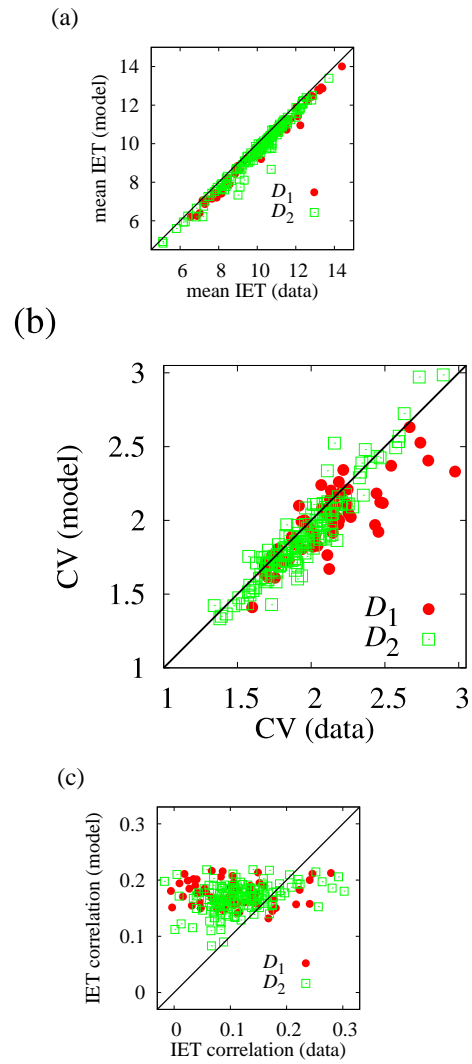


Fig. 7 Comparison between the data and the estimated model. (a) mean IET, (b) CV, and (c) IET correlation. Each data point corresponds to one valid individual. The mean IET, CV, and IET correlation for the data are calculated on the basis of the days containing at least 40 events.

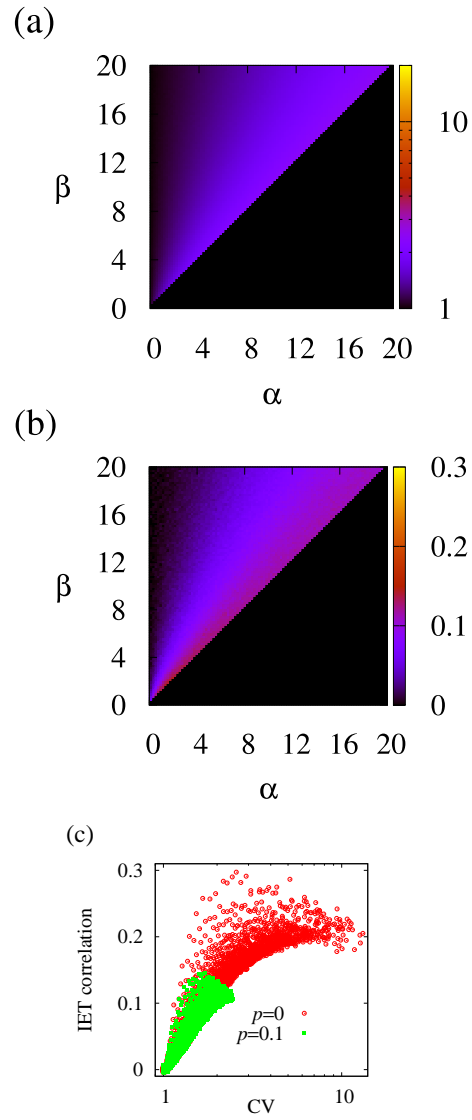


Fig. 8 Results for the modified Hawkes process with $\nu = 1$. (a) CV with $p = 0.1$. (b) IET correlation with $p = 0.1$. (c) Relationship between the CV and IET correlation with $p = 0$ and $p = 0.1$.